Rho Resonance Parameters from Lattice QCD

Dehua Guo, Andrei Alexandru, Raquel Molina and Michael Döring

Jefferson Lab Seminar

Oct 03, 2016

Overview

Introduction to Lattice QCD

- Most visible matter in the universe are made up of particles called hadrons.

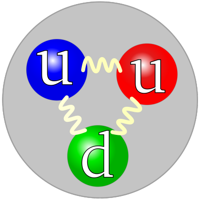

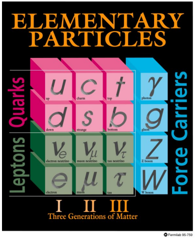

- The interaction between hadrons is dominated by the strong force.
- Quantum Chromodynamics (QCD) is a theory to describe the strong interaction between quarks and gluons which make up hadrons.

$$\mathcal{L}_{QCD} = -\frac{1}{2}\,\mathrm{Tr}\,F_{\mu\nu}F^{\mu\nu} - \sum_f \bar{\psi}_f \gamma^\mu \left[\partial_\mu - igA_\mu\right]\psi_f - \sum_f m_f \bar{\psi}_f \psi_f, \qquad (1)$$

- Some techniques to work with QCD: Perturbation theory, Effective field theory, Lattice QCD and so on.

Introduction to Lattice QCD

For light hadron study, non-perturbative approach is needed. Lattice QCD is a non-perturbative approach to QCD. It formulates QCD in a discrete way.

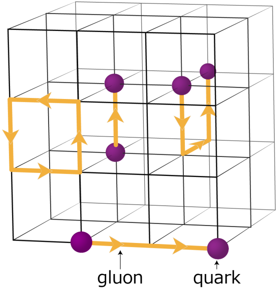

Inputs:

- lattice geometry N
- lattice spacing a set indirectly through the coupling constant g
- quark mass represented by pion mass m_π

For light hadron study, only light quarks u and d are important. s quark introduces only small correction.
The role of Lattice QCD in resonance study is to extract the energy spectrum for two hadron states.

Introduction to Lattice QCD

Why we study resonances from Lattice QCD?

- Lattice QCD offers us a way to study the resonances in terms of quark and gluon dynamics. It serves as a test of QCD for well determined resonance parameters.
- The techniques can be used to investigate systems where the experimental situation is less clear.
- Validate effective models used to describe hadron scattering.

How?

- We start from meson resonance because they have better signal-to-noise ratio.
- $\rho(770)$ resonance in $I = 1, J = 1$ π-π scattering channel.

Symmetries on the lattice

On the lattice, the energy eigenstates $|n>$ of the system are computed in a given irrep of the lattice symmetry group.

$$\psi_n(R^{-1}x) = \psi_n(R^{-1}(x + \mathbf{n}L)); \qquad \left\langle \hat{O}_2(t)\hat{O}_1^\dagger(0) \right\rangle = \sum_n \left\langle 0|\hat{O}_2|n \right\rangle \left\langle n|\hat{O}_1|0 \right\rangle e^{-tE_n} \quad (2)$$

Isospin, color and flavor symmetries are similar to the continuum.

Table: Irreducible representation in $SO(3), O$ and D_4

	$SO(3)$	cubic box(O_h)	elongated box(D_{4h})
irep label	$Y_{lm}; l = 0, 1...\infty$	A_1, A_2, E, F_1, F_2	A_1, A_2, E, B_1, B_2
dim	$1, 3, ..., 2l + 1, ...\infty$	$1, 1, 2, 3, 3$	$1, 1, 2, 2, 2$

Table: Angular momentum mixing among the irreducible representations of the lattice group

O_h		D_{4h}	
irreducible representation	l	irreducible representation	l
A_1	0,4,6, ...	A_1	0,2,3, ...
A_2	3,6, ...	A_2	1,3,4, ...
F_1	1,3,4,5,6, ...	B_1	2,3,4, ...
F_2	2,3,4,5,6, ...	B_2	2,3,4, ...
E	2,4,5,6, ...	E	1,2,3,4, ...

Symmetries of the elongated box

ρ resonance is in $I = 1, J^P = 1^-$ channel for pion-pion scattering. Elongated box method tunes the momentum of the scattering particles on the lattice $\mathbf{p} \propto (\frac{2\pi}{\eta L})$.

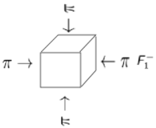

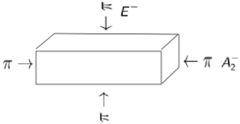

The $SO(3)$ symmetry group reduce to discrete subgroup O_h or D_{4h}

J	O_h	D_{4h}
0	A_1^+	A_1^+
1	F_1^-	$A_2^- \oplus E^-$
2	$E^+ \oplus F_2^+$	$A_1^+ \oplus B_1^+ \oplus B_2^+ \oplus E^+$
3	$A_2^- \oplus F_1^- \oplus F_2^-$	$A_2^- \oplus B_1^- \oplus B_2^- \oplus 2E^-$
4	$A_1^+ \oplus E^+ \oplus F_1^+ \oplus F_2^+$	$2A_1^+ \oplus A_2^+ \oplus B_1^+ \oplus B_2^+ \oplus 2E^+$

For the p-wave($l = 1$) scattering channel, we only need to construct the interpolating fields in F_1^- in the O_h group, A_2^- representations in D_{4h} group because the energy contribution from angular momenta $l \geq 3$ is negligible.

Lüscher's formula for elongated box [1]

Phase shift for $I = 1$, rest frame ($\mathbf{P} = 0$):

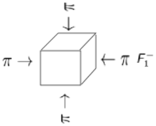

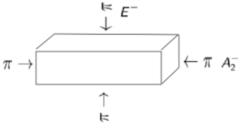

$$A_2^- : \cot\delta_1(k) = \mathcal{W}_{00} + \frac{2}{\sqrt{5}}\mathcal{W}_{20} \tag{3}$$

$$\tag{4}$$

$$\mathcal{W}_{lm}(1, q^2, \eta) = \frac{\mathcal{Z}_{lm}(1, q^2, \eta)}{\eta\pi^{\frac{3}{2}} q^{l+1}}; \quad q = \frac{kL}{2\pi}; \ \eta = \frac{N_{el}}{N} : \text{elongation factor} \tag{5}$$

Zeta function

$$\mathcal{Z}_{lm}(s; q^2, \eta) = \sum_{\tilde{\mathbf{n}}} \mathcal{Y}_{lm}(\tilde{\mathbf{n}})(\mathbf{n}^2 - q^2)^{-s}; \ \mathbf{n} \in \mathbf{m} \tag{6}$$

Total energy

$$E = 2\sqrt{m^2 + k^2}; \quad k = \sqrt{\left(\frac{E}{2}\right)^2 - m^2} \tag{7}$$

[1] X. Feng, X. Li, and C. Liu, Phys.Rev. D70 (2004) 014505

Lüscher's formula for boost frame

In order to obtain new kinematic region, we boost the resonance along the elongated direction.

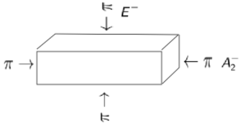

$$\mathbf{P} \rightarrow$$

$$A_2^- : \cot \delta_1(k) \quad = \quad \mathcal{W}_{00} + \frac{2}{\sqrt{5}} \mathcal{W}_{20} \tag{8}$$

$$\tag{9}$$

$$\mathcal{W}_{lm}(1, q^2, \eta) = \frac{\mathcal{Z}_{lm}^{\mathbf{P}}(1, q^2, \eta)}{\gamma \eta \pi^{\frac{3}{2}} q^{l+1}}; \quad \eta = \frac{N_{el}}{N} \text{ : elongation factor; } \; \gamma \text{ : boost factor;} \tag{10}$$

$$\mathcal{Z}_{lm}^{\hat{\mathbf{P}}}(s; q^2, \eta) = \sum_{\mathbf{n}} \mathcal{Y}_{lm}(\tilde{\mathbf{n}})(\tilde{\mathbf{n}}^2 - q^2)^{-s}; \mathbf{n} \in \frac{1}{\gamma}(\mathbf{m} + \frac{\hat{\mathbf{P}}}{2}); \tag{11}$$

Interpolating field construction for ρ resonance

Four $q\bar{q}$ operators and two scattering operators $\pi\pi$ in A_2^- sector.

$$\rho^J(t_f) = \bar{u}(t_f)\Gamma_{t_f} A_{t_f}(\mathbf{p}) d(t_f); \quad \rho^{J\dagger}(t_i) = \bar{d}(t_i)\Gamma^\dagger_{t_i} A^\dagger_{t_i}(\mathbf{p}) u(t_i) \tag{12}$$

N	Γ_{t_f}	A_{t_f}	$\Gamma^\dagger_{t_i}$	$A^\dagger_{t_i}$
1	γ_i	$e^{i\mathbf{p}}$	$-\gamma_i$	$e^{-i\mathbf{p}}$
2	$\gamma_4\gamma_i$	$e^{i\mathbf{p}}$	$\gamma_4\gamma_i$	$e^{-i\mathbf{p}}$
3	γ_i	$\nabla_j e^{i\mathbf{p}} \nabla_j$	γ_i	$\nabla_j^\dagger e^{-i\mathbf{p}} \nabla_j^\dagger$
4	$\frac{1}{2}$	$\{e^{i\mathbf{p}}, \nabla_i\}$	$-\frac{1}{2}$	$\{e^{-i\mathbf{p}}, \nabla_i\}$

$$(\pi\pi)_{\mathbf{P},\Lambda,\mu} = \sum_{\mathbf{p_1}^*,\mathbf{p_2}^*} C(\mathbf{P},\Lambda,\mu;\mathbf{p_1};\mathbf{p_2})\pi(\mathbf{p_1})\pi(\mathbf{p_2}), \tag{13}$$

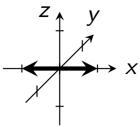

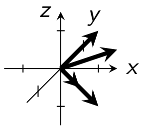

$$\pi\pi_{100}(\mathbf{p_1},\mathbf{p_2},t) = \frac{1}{\sqrt{2}}[\pi^+(\mathbf{p_1})\pi^-(\mathbf{p_2}) - \pi^+(\mathbf{p_2})\pi^-(\mathbf{p_1})]; \quad \mathbf{p_1} = (1,0,0) \quad \mathbf{p_2} = (-1,0,0)$$

$$\pi\pi_{110} = \frac{1}{2}(\pi\pi(110) + \pi\pi(101) + \pi\pi(1-10) + \pi\pi(10-1))$$

6×6 correlation matrix

$$C = \begin{pmatrix} C_{\rho^J \leftarrow \rho^{J'}} & C_{\rho^J \leftarrow \pi\pi_{100}} & C_{\rho^J \leftarrow \pi\pi_{110}} \\ C_{\pi\pi_{100} \leftarrow \rho^{J'}} & C_{\pi\pi_{100} \leftarrow \pi\pi_{100}} & C_{\pi\pi_{100} \leftarrow \pi\pi_{110}} \\ C_{\pi\pi_{110} \leftarrow \rho^{J'}} & C_{\pi\pi_{110} \leftarrow \pi\pi_{100}} & C_{\pi\pi_{110} \leftarrow \pi\pi_{110}} \end{pmatrix}. \quad (14)$$

The correlation functions: $\bar{u}(t_i) \longrightarrow u(t_f)$

$\Gamma^J_{t_f}, (\mathbf{p}, t_f)$

$C_{\rho_i \leftarrow \rho_j} = -\Big\langle$  $\Big\rangle = -\left\langle \mathrm{Tr}[M^{-1}(t_i, t_f)\Gamma^J_{t_f} e^{i\mathbf{p}} M^{-1}(t_f, t_i)\Gamma^{J'\dagger}_{t_i} e^{-i\mathbf{p}}] \right\rangle.$ (15)

$\Gamma^{J'\dagger}_{t_i}, (-\mathbf{p}, t_i)$

$C_{\rho_i \leftarrow \pi\pi} = \Big\langle$ 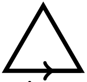 $-$ 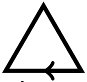 $\Big\rangle \overset{\mathbf{P}=0}{\equiv} 2 \Big\langle$ 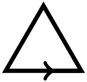 $\Big\rangle.$ (16)

$C_{\pi\pi \leftarrow \pi\pi} = -\Big\langle$ 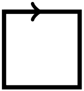 $+$ 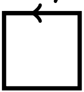 $-$ 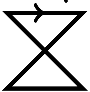 $-$ 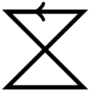 $+$  $-$   $\Big\rangle$ (17)

$\overset{\mathbf{P}=0}{\equiv} - \Big\langle 2$ 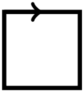 $-\, 2$ 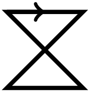 $+$  $-$   $\Big\rangle$ (18)

Laplacian Heaviside smearing [2]

To estimate all-to-all propagators: 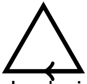 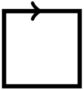

The 3-dimensional gauge-covariant Laplacian operator

$$\tilde{\Delta}^{ab}(x,y;U) = \sum_{k=1}^{3} \left\{ \tilde{U}_k^{ab}(x)\delta(y,x+\hat{k}) + \tilde{U}_k^{ba}(y)^*\delta(y,x-\hat{k}) - 2\delta(x,y)\delta^{ab} \right\}. \tag{19}$$

$$S_\Lambda(t) = \sum_{\lambda(t)}^{\Lambda} |\lambda(t)\rangle \langle\lambda(t)| \, ; \quad \tilde{u}(t) = S(t)u(t) = \sum_{\lambda_t} |\lambda_t\rangle \langle\lambda_t| \, u(t). \tag{20}$$

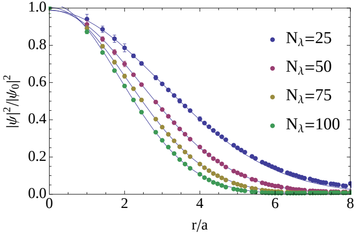

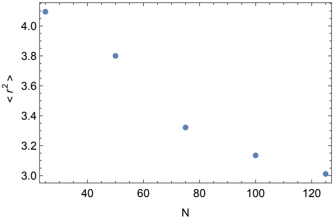

[2] C. Morningstar, J. Bulava, J. Foley, K. J. Juge, D. Lenkner, et al., Phys.Rev. D83 (2011) 114505

Energy spectrum

We implement the calculation in 3 ensembles ($\eta = 1.0, 1.25, 2.0$) at $m_\pi \approx 310\,\text{MeV}$ and 3 ensembles ($\eta = 1.0, 1.17, 1.33$) at $m_\pi \approx 227\,\text{MeV}$ with nHYP-smeared clover fermions and two mass-degenerated quark flavor.

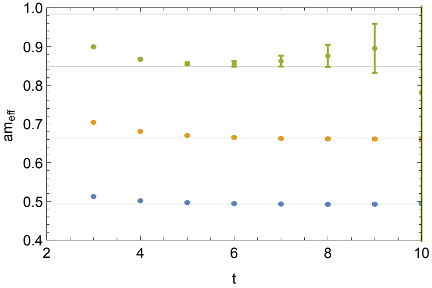

Figure: The lowest three energy states with their error bars for $\eta = 1.0$, $m_\pi = 310\,\text{MeV}$ ensemble

We extract energy E by using double exponential $f(t) = we^{-Et} + (1-w)e^{-E't}$ to do the χ^2 fitting for each eigenvalues.

Energy spectrum

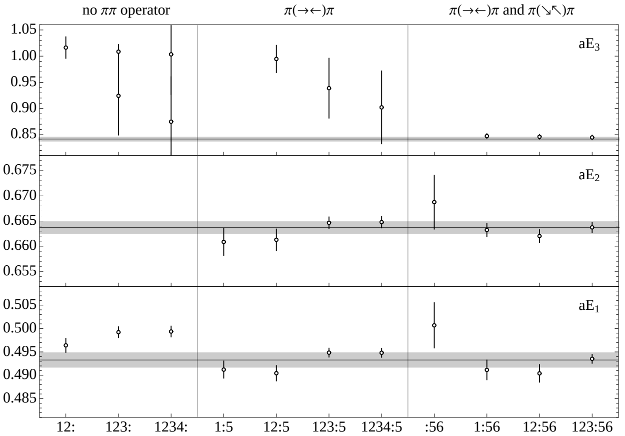

$\mathcal{O}_i$	1	2	3	4	5	6
	ρ_1	ρ_2	ρ_3	ρ_4	$\pi\pi_{100}$	$\pi\pi_{110}$

(21)

Expectation for energy states

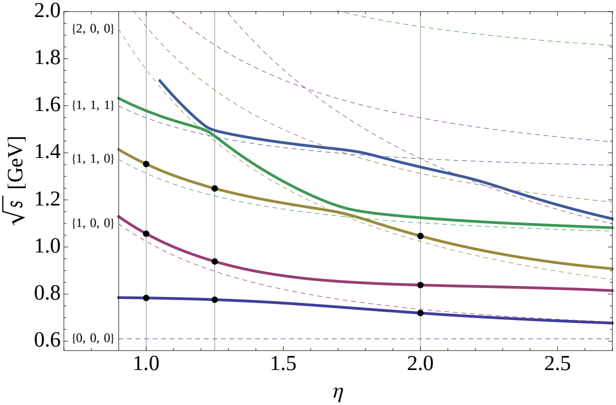

Figure: The lowest 3 energy states prediction fromUχPTmodel. When $\eta = 2.0$ the 3*rd* state is from operator $\pi\pi_{200}$ instead of $\pi\pi_{110}$

Phaseshift fitted with Breit Wigner Form

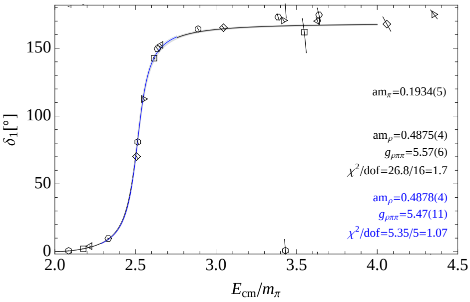

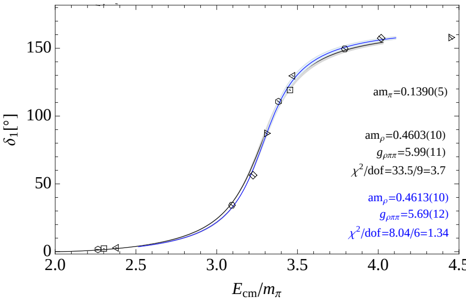

$$\cot(\delta_1(E)) = \frac{M_R^2 - E^2}{E\Gamma_r(E)}, \quad \Gamma_r(E) \equiv \frac{g_{R12}^2}{6\pi}\frac{p^3}{E^2}. \tag{22}$$

$$\delta_1(E) = \text{arccot}\, \frac{6\pi(M_R^2 - E^2)E}{g^2 p^3} \tag{23}$$

Phaseshift fitted with UχPTmodel

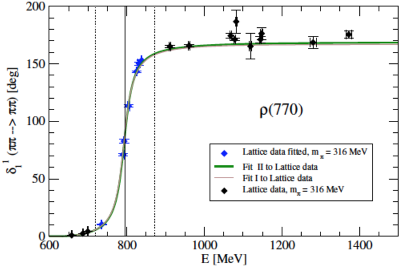

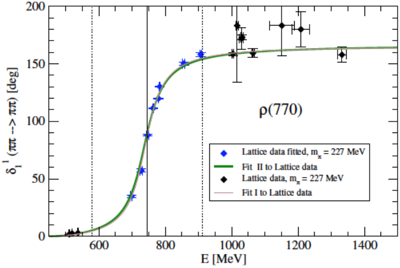

Figure: $m_\pi \approx 315\,\text{MeV}$ and $m_\pi \approx 227\,\text{MeV}$ data fitted with UχPT model.

	m_π	m_ρ	Γ_ρ	g	χ^2/dof
Breit Wigner	315	794.6(6)	37.0(2)	5.57(11)	2.16
UχPT		795.2(3)	36.1(1)		1.26
Breit Wigner	227	748.4(1.6)	71.0(8)	5.70(12)	1.46
UχPT		748.2(7)	77.0(5)		1.53

$K\bar{K}$ channel contribution to ρ resonance

We study the $K\bar{K}$ effect using UχPTmodel with input parameters m_π, f_π, f_K and low energy constant $\hat{l}_{1,2}$.

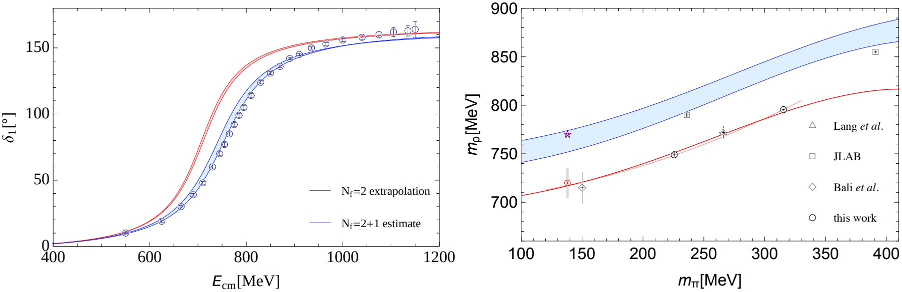

Figure: (Left) Chiral extrapolation of the phase shift to the physical mass (red band), obtained from the simultaneous fit to pion masses. The blue band: phaseshift with $K\bar{K}$. Open circles: experiment data [3]

m_ρ and $g_{\rho\pi\pi}$ comparison

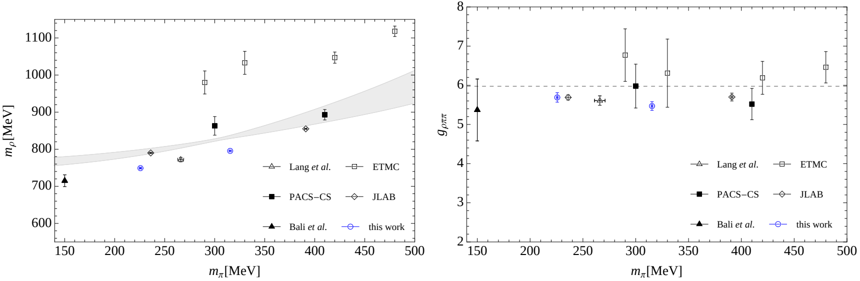

Figure: Comparison of different lattice calculation for the ρ resonance mass (left) and width parameter $g_{\rho\pi\pi}$ (right). The errors included here are only stochastic. The band in the left plot indicates a $N_f = 2+1$ expectation from UχPT model constrained by some older lattice QCD data and some other physical input [4].

The results of ETMC are taken from [5]. PACS result is from [6].

Conclusions

- We complete a precision study of ρ resonance with LapH smearing method and obtain the resonance parameters at $m_\pi \approx 310\,\text{MeV}$ and $m_\pi \approx 227\,\text{MeV}$.
- For precise energy spectrum results, both Breit Wigner form and UχPTmodel work well in the resonance region. Modification to the BW is needed when applied to a wider energy region.
- The extrapolation of m_ρ to physical pion mass is smaller than $m_\rho^{\text{phy}} = 775\,\text{MeV}$ in a $N_f = 2$ situation, we believe that this comes from the absence of strange quark and the $K\bar{K}$ channel which is supported by our UχPTstudy.

X. Feng, X. Li, and C. Liu, *Two particle states in an asymmetric box and the elastic scattering phases*, *Phys.Rev.* **D70** (2004) 014505, [hep-lat/0404001].

C. Morningstar, J. Bulava, J. Foley, K. J. Juge, D. Lenkner, et al., *Improved stochastic estimation of quark propagation with Laplacian Heaviside smearing in lattice QCD*, *Phys.Rev.* **D83** (2011) 114505, [arXiv:1104.3870].

S. D. Protopopescu, M. Alston-Garnjost, A. Barbaro-Galtieri, S. M. Flatte, J. H. Friedman, T. A. Lasinski, G. R. Lynch, M. S. Rabin, and F. T. Solmitz, *Pi pi Partial Wave Analysis from Reactions pi+ p —¿ pi+ pi- Delta++ and pi+ p —¿ K+ K- Delta++ at 7.1-GeV/c*, *Phys. Rev.* **D7** (1973) 1279.

J. R. Pelaez and G. Rios, *Chiral extrapolation of light resonances from one and two-loop unitarized Chiral Perturbation Theory versus lattice results*, *Phys. Rev.* **D82** (2010) 114002, [arXiv:1010.6008].

X. Feng, K. Jansen, and D. B. Renner, *Resonance Parameters of the rho-Meson from Lattice QCD*, *Phys.Rev.* **D83** (2011) 094505, [arXiv:1011.5288].

PACS Collaboration, S. Aoki et al., *ρ Meson Decay in 2+1 Flavor Lattice QCD*, *Phys. Rev.* **D84** (2011) 094505, [arXiv:1106.5365].

P. Estabrooks and A. D. Martin, *pi pi Phase Shift Analysis Below the K anti-K Threshold*, *Nucl. Phys.* **B79** (1974) 301.

Symmetries on the lattice

The $SO(3)$ symmetry group reduce to discrete subgroup O_h or D_{4h}

Table: Resolution of $2J+1$ spherical harmonics into the irreducible representations of O_h and D_{4h}

J	O_h	D_{4h}
0	A_1^+	A_1^+
1	F_1^-	$A_2^- \oplus E^-$
2	$E^+ \oplus F_2^+$	$A_1^+ \oplus B_1^+ \oplus B_2^+ \oplus E^+$
3	$A_2^- \oplus F_1^- \oplus F_2^-$	$A_2^- \oplus B_1^- \oplus B_2^- \oplus 2E^-$
4	$A_1^+ \oplus E^+ \oplus F_1^+ \oplus F_2^+$	$2A_1^+ \oplus A_2^+ \oplus B_1^+ \oplus B_2^+ \oplus 2E^+$

Assume that the energy contribution from angular momenta $l \geq 3$ is negligible. For example, if we study the p-wave($l = 1$) scattering channel, we should construct the interpolating field in F_1^- in the O_h group, A_2^- and E^- representations in D_{4h} group.

Variational method [?]

Variational method is used to extract energy of the excited states.
Construct correlation matrix in the interpolator basis

$$C(t)_{ij} =< \mathcal{O}_i(t)\mathcal{O}_j^\dagger(0) >; i,j = 1,2,..., \text{number of operators} \quad (24)$$

The eigenvalues of the correlation matrix are

$$\lambda^{(n)}(t,t_0) \propto e^{-E_n t}(1+\mathcal{O}(e^{-\Delta E_n t})), n = 1,2,..., \text{number of operators} \quad (25)$$

where $\Delta E_n = E_{\text{Number of operators } + 1} - E_n$.

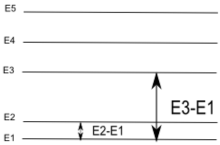

Larger energy gap makes the high lying energy decay faster and effective mass plateau appear in an earlier time slice.

Appendix-B: LapH smearing

Benefit from LapH smearing:

- Keep low frequency mode up to Λ cutoff to compute the all to all propagators, $u(x) \longrightarrow u(y)$. The number of propagators $M^{-1}(t_f, t_i)$ need to be computed reduce from 6.34×10^{13} in position space to 3.7×10^{8} in momentum space for the $24^3 48$ ensemble.
- The effective mass reach a plateau in an earlier time slice.

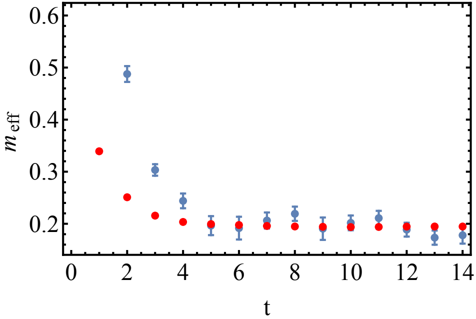

Figure: pion effective mass with (red) and without LapH smearing (blue)

Appendix-C: Fitting phase-shift

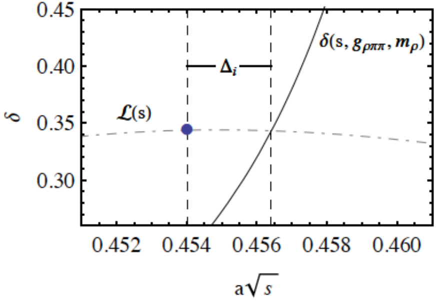

Figure: χ^2 fitting for the phase shift data to Breit Wigner form

$$\chi^2 = \Delta^T COV^{-1} \Delta \tag{26}$$

where

$$\Delta_i = \sqrt{s_i^{\text{curve}}} - \sqrt{s_i^{\text{data}}} \tag{27}$$

Appendix-D: Experiment data [7]

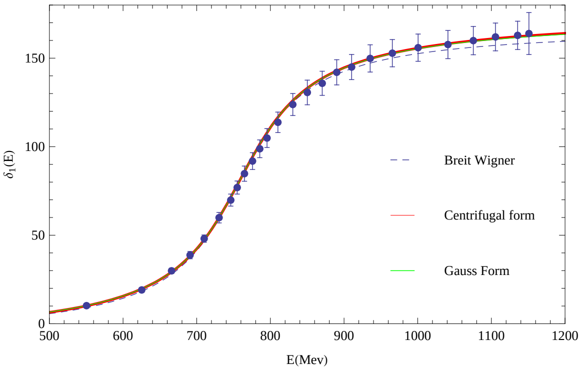

$$\Gamma_{BW}(E) = \frac{g^2}{6\pi}\frac{p^3}{E^2}$$

$$\Gamma_{CF}(E) = \frac{g^2}{6\pi}\frac{p^3}{E^2}\frac{1+(p_R R)^2}{1+(pR)^2}$$

$$\Gamma_{GA}(E) = \frac{g^2}{6\pi}\frac{p^3}{E^2}\frac{e^{-p^2/6\beta^2}}{e^{-p_R^2/6\beta^2}}$$

Figure: $\pi\pi$ phase shift below $K\bar{K}$ threshold in experiment

[7] Estabrooks, P. and Martin, Alan D. Nucl.Phys. B79 (1974) 301

K-matrix method

$$T^{-1} = V^{-1} - G = \frac{-3(f^2 - 8l_1 m_\pi^2 + 4l_2 W^2)}{2p^2} - \mathrm{Re}G(W) + \frac{ip}{8\pi W} \tag{28}$$

For K-matrix method the $\mathrm{Re}G(W) = 0$.

$$T = \frac{-8\pi W}{p\cot\delta p - ip} \tag{29}$$

$$l_1 = \frac{1}{8\pi^2}\left(-\frac{1}{2}\frac{m_\rho^2}{g_{\rho\pi\pi}^2} + f^2\right) \tag{30}$$

$$l_2 = -\frac{1}{8g_{\rho\pi\pi}^2} \tag{31}$$